Recent rise of water levels of Lake Nakuru, Kenya: Unraveling the Changing Precipitation Regime and its Climatic Drivers

R. Ampting[1], R. van der Ent[1], V. Kiluva[2], N. van de Giesen[1]

[1]Delft University of Technology, The Netherlands
[2]Masinde Muliro University of Science and Technology, Kenya

Key Points:

- A significant positive change point of annual precipitation has been detected for the lake Nakuru catchment, Kenya, in 2010.
- Rising water levels can be attributed to an increase in precipitation, especially in April and September.
- The precipitation regime changes are associated with a southward shift in Indian Ocean moisture sources and rising sea surface temperatures.

Corresponding author: Nick van de Giesen, `N.C.vandeGiesen@tudelft.nl`

Abstract

The Kenyan Rift Valley has experienced an abrupt and significant rise in its lake levels since 2010, followed by a more rapid rise since 2020. This paper examines the dynamic changes in precipitation patterns and their climatic drivers in the Kenyan Rift Valley region from 1981 to 2021, focusing on Lake Nakuru. Notably, in 2010, a pivotal change point in precipitation aligns with the rising water levels of Lake Nakuru. Using an atmospheric moisture tracking model, our study reveals that this transformation is associated with a southward shift in moisture sources. More moisture is now coming from the southern Indian Ocean, where substantial increases in sea surface temperatures and evaporation are observed. These findings highlight the complex interplay between climatic drivers, changing moisture sources, and lake Nakuru's water levels.

Plain language summary

This research paper explores the reasons behind the recent flooding of the shores of Lake Nakuru in Kenya, which displaced thousands of people. The study investigates whether the lake's rising water levels are primarily caused by changes in the climate and increased rainfall. Data is used from various sources, including weather stations, lake measurements, and climate data. Since 2010, a significant increase in rainfall was found in the Lake Nakuru catchment area, especially in the months of April and September. This increase in rainfall was the main cause of the lake's expansion. Our model tracked raindrops backwards in time as moisture to its origin from where the water evaporated. In recent years, there has been a shift in moisture sources, with more moisture coming from the land and the coastal sea. This change is linked to rising sea surface temperatures in the Indian Ocean. These findings emphasize the significant role of climate change in shaping the hydrology of lake Nakuru region as part of the Kenyan Rift Valley and its impact on the lake's water levels.

1 Introduction

The hydro-meteorological system of Eastern African, and more specifically the Kenyan Rift Valley, is quite complex and dynamic. Changes in the hydrology of the lakes (Dyer & Washington, 2021; Gichuru & Waithaka, 2016) and the impact of climate change (Black et al., 2003; Black, 2005) have become indisputable in recent decades. Interestingly, and unfortunately, lakes in the Kenyan Rift Valley region, from the south to the north of Kenya, have been experiencing an increase in their water levels resulting in severe flooding. There is an abrupt change in lake behavior with a steady rise throughout the 2010s (Herrnegger et al., 2021).

Precipitation in Eastern Africa and Kenya is highly variable and seasonal. Four seasons can be distinguished, namely, the dry season (JF), the long rainy season (MAM), the continental rainy season (JJAS), and the short rainy season (OND) (Dyer & Washington, 2021; Yang et al., 2015). Inter-annual variations are common and an average increase in precipitation has been observed since 2010 (Dyer & Washington, 2021; Gichuru & Waithaka, 2016; Herrnegger et al., 2021; Kimaru et al., 2019). Herrnegger et al. (2021) explore the relationship between precipitation and lake characteristics on a annual basis for all lakes in the Rift Valley and found a relationship between rainfall surplus and deficits with lake surface area fluctuations.

The origin of East African precipitation is highly dynamic and dictated by numerous climatic influences. This geographic area receives moisture from three major air systems, the northeastern monsoon system and the southeastern monsoon system from the Indian Ocean, and South Westerly humid air from the Congo basin (Balagizi et al., 2018). The seasonality of precipitation is governed by the interchange between the two monsoon systems. The relative and locational shift in moisture source evaporation that contributes to precipitation to the lake Nakuru catchment, hereafter named evaporative contribution, is unknown.

The objective of this research is to gain insights into changes in moisture sources and their evaporative contribution as possible cause for the rising water levels in lake Nakuru. We do so by using a widely used atmospheric moisture tracking method WAM2layers (Carr & Ummenhofer, 2023; Guo et al., 2019; Benedict et al., 2020; Liu et al., 2021; Duerinck et al., 2016; R. J. Van der Ent & Savenije, 2013; Keys et al., 2022), which allows us to identify changes and variability in precipitation and its origin. These interrelations could provide insights into the impact on future precipitation regime changes.

2 Materials and methods

2.1 Site description

Kenya is situated in East Africa and is characterized by two rainy seasons and has a mean annual precipitation of 703 mm (The World Bank Group, 2021). Precipitation in Kenya originates from the Indian Ocean, as low-level mean winds from southeastern direction move over Kenya between June and August, and shift direction to a more northeasterly wind between December and February, subject to the Inter Tropical Convergence Zone (ITCZ) (Levin et al., 2009). The ITCZ separates northerly and southerly air flows, whereas the Congo Air Boundary separates westerly flow from easterly low-level flows. The interplay between the two boundaries determines the meteorological situation in Kenya. As a result, precipitation throughout the year experiences different contributing regions as wind patterns and SST gradients shift with the ITCZ.

In addition to these meteorological influences, the topography of Kenya is a key determinant of its complex meteorological system. High altitude plateaus between 1000 and 2000 m are interspersed by mountains of over 4000m, causing unique weather patterns for different areas. The Rift Valley runs from the South of Kenya to the North and has a complex topography ranging from 3700 m in the south, to 300 m in the north. The complexity is important for the dynamic precipitation regimes in the Kenyan Rift Valley. One of many lakes in the Rift Valley is lake Nakuru, the region of interest for this research.

The lake Nakuru catchment is visualized in Figure 1. It is a salt water lake and situated at 1760 m above sea level with a catchment area of about 1600 km^2 lying in a closed hydrological basin along the southeastern escarpment of the Kenyan Rift Valley. It experiences a mean precipitation of 892 mm/year (see Figure 2a). Lake Nakuru has a surface area between 30 and 60 km^2 and varying depth between 0.5 and 8 m (Schwatke et al., 2019; Iradukunda et al., 2020). Due to its shallowness, the lake is sensitive to climatic variations as it has little buffer capacity to withstand inter- and intra-seasonal variability and experiences high evaporation rates. During the drought years of 1993 and 1996 this resulted in the lake almost drying out, while during wet years like 1997 and 2019 the lake has experienced major flooding (ilec, 2005; Kimaru et al., 2019; Odada, 2001).

2.2 Materials

The Kenya Meteorological Department (KMD) provided precipitation data of fourteen weather stations, from 1981 to 2021, divided over the catchment area (Figure 1) (KMD, 2022). The data provided by KMD did not reveal any data gaps, indicating the KMD processed their data before sharing. Figure 1 visualizes the catchment area with weather station locations.

The Thiessen polygon method was applied to determine the catchment average precipitation and lake precipitation (Schumann, 1998). Lake precipitation was defined by weather stations 6, 7, 10, and 11, considering contributing area. A more sophisticated method would

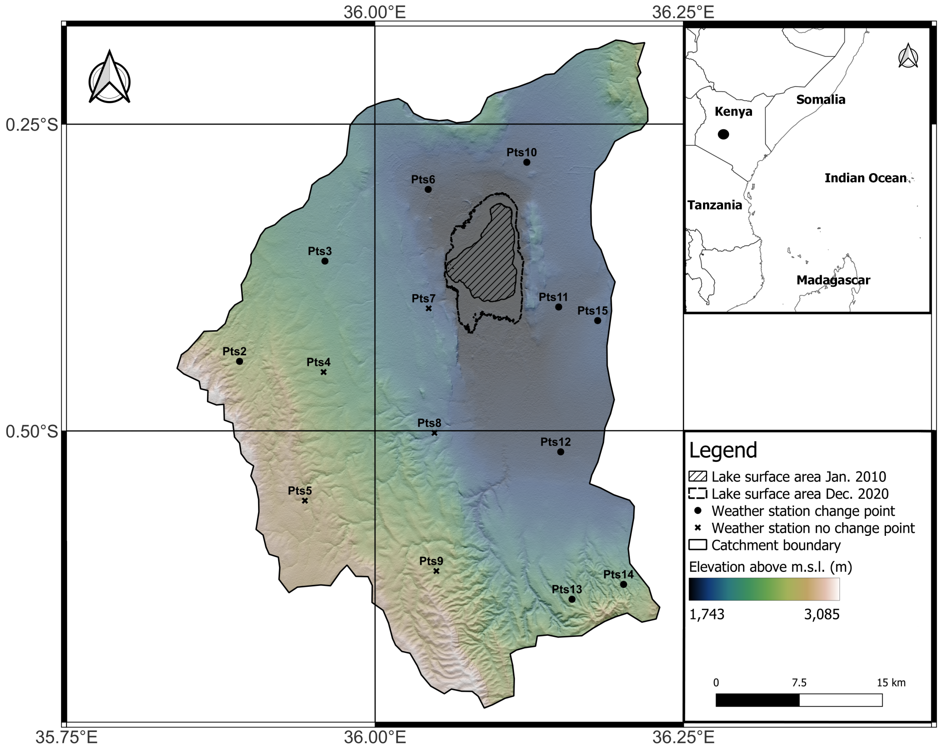

Figure 1. Representation of the Lake Nakuru catchment in Kenya (Latitude: 0.357 S, Longitude: 36.092 E), illustrating the location of the lake boundaries in December 2020 (maximum) and January 2010 (minimum), along with the location of 14 precipitation stations (Pts).

not have a large impact on outcome of this research since only monthly and annual precipitation are used. Detailed information on the weather station locations and Thiessen area weight can be found in Table S1.

The datasets used to derive lake behavior are the Database for Hydrological Time Series of Inland Waters (DAHITI) (Schwatke et al., 2019), and a bathymetry study with echo-sounding technology performed by Jomo Kenyatta University of Agriculture and Technology (JKUAT) (Iradukunda et al., 2020). The minimum and maximum surface area contours, around January 2010 and December 2020 respectively, are shown in Figure 1. The bathymetry study reveals a certain relation between lake surface area and volume. By combining this with the DAHITI time series it is possible to construct a time series for the lake volume as well.

The moisture tracking model WAM2layers was forced with ERA5 hourly data (ERA5, 2017; Hersbach, 2023). We used the following input variables: total precipitation, evaporation, surface pressure, total column of water, specific humidity, and u and v component of wind. We downloaded the data on the domain 40° S to 40° N, 0°to 100° E between 1981 and 2021 . The model level data comprises 22 model levels and a grid size of $0.5° \times 0.5°$.

Sea surface temperature (SST) is used in this research to assess the impact on different moisture sources. The European Center for Medium-Range Weather Forecasts provides the Ocean Reanalysis System 5 (Copernicus, 2021). It combines model data with observations globally covering 1979 to present at a resolution of $0.25° \times 0.25°$.

2.3 Lake characteristics and precipitation regime

Here, we validate the change point in precipitation regime, that was found in 2010 by earlier studies (Herrnegger et al., 2021). The detection method for validating change points we us is the Ruptures package introduced by Truong et al. (2020). The algorithm takes a time series signal as input, where the goal is to find the optimal segmentation. It uses a built-in cost function. The cost function represents the criterion used to measure the quality of a segmentation or breakpoint. We used the L2 cost function, also known as the squared error cost function. The minimum size of the segment is set to 10 years under the assumption that only 1 breakpoint is present in the data. A recursive algorithm finds the optimal segmentation. The algorithm calculates the minimum cost for all possible segments up to that time. The algorithm backtracks to recover the years of the point of change once the optimal segmentation is found.

The relation between different variables is tested by the Pearson correlation at significance $p < 0.05$. To test if a change point is significant the Mann-Whitney U (MW) test (McKnight & Najab, 2010) at significance $p < 0.05$ is used. The MW test, also known as the Wilcoxon rank-sum test, does not assume a normal distribution and is suitable for smaller data sets. It also assumes two sub-samples were extracted from a larger sample of the same population. If the segmentation is proven significant, the first year after the year of change is called a change point. Liang et al. (2011) applied the method to find jumps in precipitation time series in the northeast of China and Keim and Muller (1992) investigated whether local heavy rainfall regimes had changed through the analysis of annual maximum storm series.

2.4 Moisture tracking and climatic drivers

We used the WAM2layers offline Eulerian moisture tracking model to track precipitation 10 days backward in time (R. Van der Ent et al., 2022). Precipitation is considered in the region 0.7° S to 0.2° S and 35.7° E to 36.3° S, representing the Lake Nakuru catchment. The model solves the water balance equation (Findell et al., 2019) for an upper and lower layer. Here, the water balance for tagged water in the lower layer is given by:

$$\frac{\partial S_{g,\mathrm{lower}}}{\partial t} + \frac{(S_{g,\mathrm{lower}} u)}{\partial x} + \frac{\partial (S_{g,\mathrm{lower}} v)}{\partial y} = E_g - P_g \pm F_{v,g} \qquad [L^3 T^{-1}] \tag{1}$$

With atmospheric water storage (S) computed from specific humidity and total column water data, tagged water (g), time (t), wind components (u and v), surface precipitation (P), surface evaporation (E), and vertical exchange (F_v). Vertical exchange captures moisture exchanges due to vertical wind, rainfall and rainfall re-evaporation in the atmosphere, convection, and turbulence (Van der Ent et al., 2014). A similar equation applies to the upper layer.

A distinction was made between continental and oceanic evaporative contribution to the precipitation in the catchment. The oceanic contribution was divided into ocean regions that are relevant to the time of year and moisture trajectory. In defining the ocean regions, distinctions were made between the coastal moisture sources, off the coast evaporation in the western Indian ocean, and evaporation further east in the Indian Ocean contributing to precipitation in the catchment. In this way, it is possible to identify the evaporative contribution of oceanic regions and examine possible changes. We confine our study to investigating which moisture source changes occurred in the months of April and September, which were the two months with the largest changes.

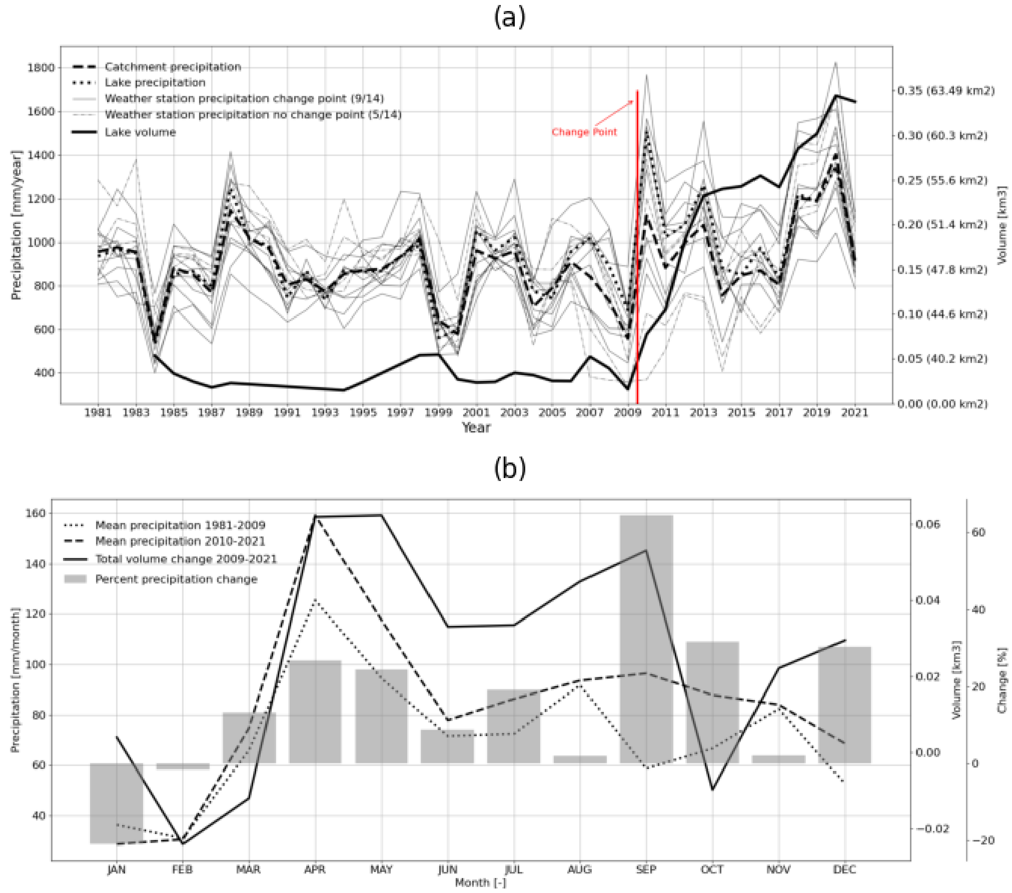

Figure 2. (a) Precipitation time series for the Lake Nakuru Catchment including lake surface area and volume. The change point is observed at 2010 for 9 out of 14 weather stations, lake precipitation and catchment precipitation. Table S2 supports the change point and significance. (b) Baseline climatology of catchment precipitation, established by averaging precipitation for each month and distinguish the time periods 1981 to 2009 and 2010 to 2021. Table S3 lists the monthly mean catchment precipitation including change point analysis.

3 Results

3.1 Lake and precipitation interaction

Figure 2a shows that both catchment precipitation and lake precipitation experienced a significant change point in 2010 as they increase 18 % and 25 %, from 849 to 1005 mm/year, and from 871 to 1091 mm/year, respectively. For individual weather stations this was true for nine out of fourteen stations (see Figure 1). The surface area and volume of the lake indicate an abrupt change in its time-series at 2010, suggesting a relation with the change point in precipitation.

January shows a decrease in precipitation while September exhibits the largest change (Figure 2b). The months April and September are responsible for 46 % of the total increase in annual catchment precipitation and exhibit an increase in precipitation of 27 % (+34 mm/month) and 64 % (+38 mm/month) after the change point. Prior to 2010, September had one of the lowest precipitation amounts, whereas in the recent period it experienced the third-highest. Notably, a change point in catchment precipitation is observed for the months September and October (see Table S3).

April, May, and September experience the highest precipitation per month after the change point year 2010 and also have the highest lake volume growth per month (Figure 2b). Three months, February, March, and October, experience on average a decline in lake volume.

Regarding monthly precipitation and lake volume change, a high positive correlation of 0.82 (p=0.00) is found in April, while a correlation of 0.26 (p=0.39) is observed in May. September precipitation demonstrates a correlation of 0.53 (p=0.06) (Table S4). April and September were investigated further as they have increased the most in absolute and relative terms regarding precipitation. These months also experienced the largest lake volume increases.

3.2 Shifts in evaporative contribution

3.2.1 April

Figure 3 shows the moisture source shift for April and September comparing prior and post 2010. In the month of April, continental evaporation contributes about 22 % (29 mm/month) on average to the total precipitation in the catchment before 2010 whereas after 2010 this is 24 % (46 mm/month). This is an increase of 56 % (17 mm/month) on average per year, while April precipitation in general only increased 27 %. This change in relative continental evaporative contribution is not marked as a change point. The Pearson correlation of precipitation to relative continental evaporative contribution intensified after the change point from 0.52 (p=0.004) to 0.78 (p=0.003) post change point. Figure S1 visualizes the overall moisture source for April.

Prior to 2010 the mean oceanic moisture contribution for April is 63 % (77 mm/month) and 64 % (93 mm/month) after 2010. This comes down to a mean absolute increase of 21 % (16 mm/month). Notably, continental evaporative contribution extends more inland as the oceanic evaporation contribution intensifies along the coast between Madagascar and Mozambique, as well as a shift in evaporative contribution to the south to the East of Madagascar (see Figure S2). Regarding the center of mass, a shift is observed to the coast and to the south (see Figure 3).

April evaporative contribution is distributed over the full Indian Ocean extending to the East of India (see Figure S1). The defined oceanic regions are listed in Table 1 and visualized in Figure S3. Three coastal regions and three oceanic regions are defined. Oceanic region 2, 5 and 6, are the most significant when it comes to evaporative contribution. After 2010, the relative contribution of oceanic regions 1, 2, 4, and 5 to oceanic evaporation has decreased, while the contribution of regions 3 and 6 has increased from 6 % to 9 % and 18 % to 21 % respectively. This indicates that the importance of regions near and north of the equator have reduced in evaporative contribution, while regions south of the equator have become more significant. Despite an overall increase in precipitation in April of 23 %, regions 1, 4, and 5 have decreased in absolute terms. Meanwhile, sea regions 2, 3, and 6 have experienced an absolute increase.

To gain further insight into the dynamics of wet and dry April months, three extreme low and high precipitation months were investigated for their moisture sources. The three driest years include 1996, 2011, and 2021, with 44 mm/month of precipitation on average. The three wettest April include 1988, 2018 and 2020, with 297 mm/month of precipitation on average (see Table 1). While the increment in precipitation average is 575 %, the increment in the absolute continental evaporative contribution is over 1250 %. On average the three driest years have continental contributions of 16 % (7 mm/month) opposed to 31 % (95

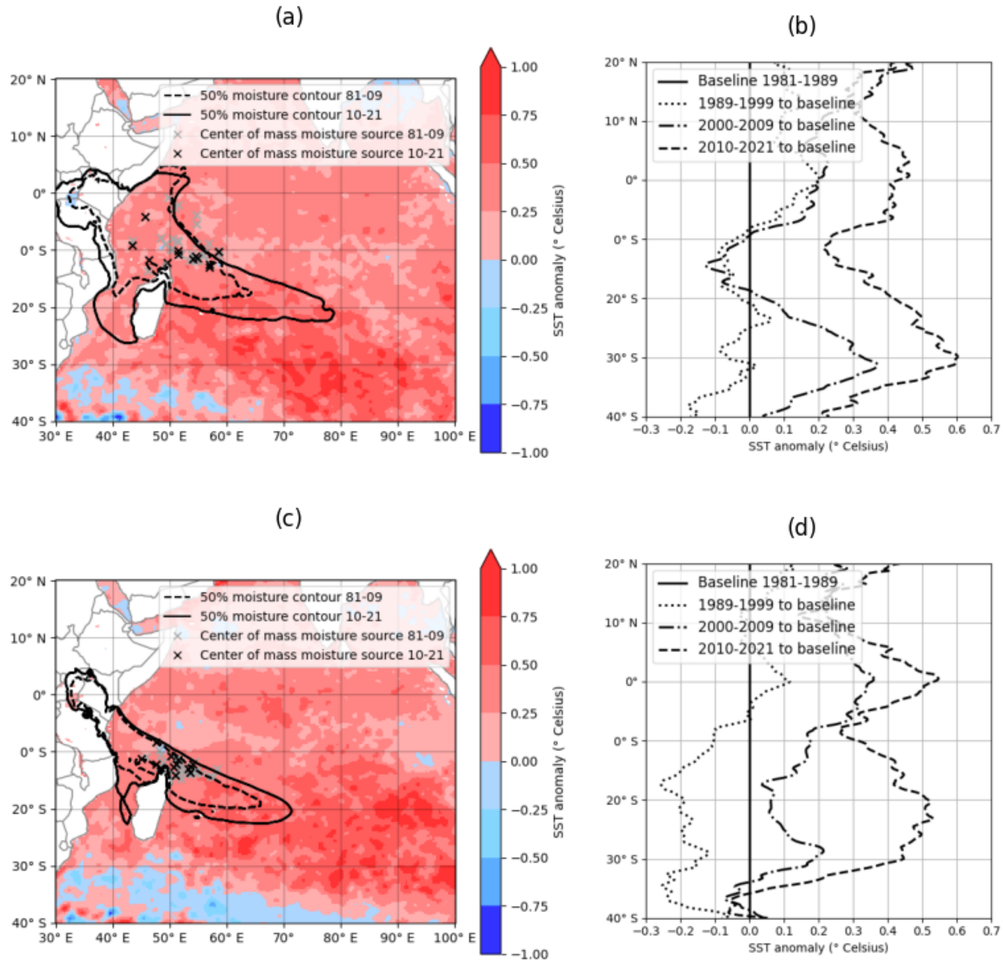

Figure 3. Difference of the mean SST for the months April (a, b) and September (c, d) both spatially (a, c) and longitudinal averaged decadal SST anomaly with respect to the baseline 1981 to 1989. Figure a and c present the 50 % of tracked moisture contour lines (averaged) and the center of mass (individual years) of the moisture sources of each year over the same time period. [9.5/12 publication units]

mm/month) in the three wettest years. In the driest and wettest months, the relative contribution of sea region 6 increased massively from 19 % to 22 %. All other regions have decreased in relative contribution.

3.2.2 September

Before 2010, in the month of September 28 % (17 mm/month) of the precipitation can be attributed to continental evaporation. Continental evaporative contribution increased to 30 % (29 mm/month) on average per month after 2010. This represents a 12 mm/month increase or a 67 % relative increase. This change in relative continental evaporative contribution is not marked as a change point. The correlation of precipitation to relative continental evaporative contribution reduced after the change point from 0.65 (p=0.000) to

Table 1. Absolute and relative contribution prior and post 2010, as well as the three driest and three wettest months of April and September. Percentages are with respect to total KMD precipitation in the catchment. The 'other' category represents evaporative contributions outside the analyzed domain. A visualization of the oceanic regions is provided in Figure S5

Source region		**1981 – 2009**	**2010 – 2021**	**Driest**	**Wettest**
April				**(1996, 2011, 2021)**	**(1988, 2018, 2020)**
Oceanic evaporative contribution					
	1. Coastal north [%]	4.3	2.4	5.2	2.4
	1. Coastal north [mm/month]	4.7	3.7	2.1	7.1
	2. Coastal equatorial [%]	16.8	16.2	19.7	14.2
	2. Coastal equatorial [mm/month]	20.1	23.0	8.6	43.6
	3. Coastal south [%]	6.1	8.9	8.2	3.7
	3. Coastal south [mm/month]	7.4	13.1	3.4	11.1
	4. Oceanic north [%]	5.3	3.5	3.5	3.2
	4. Oceanic north [mm/month]	6.0	5.6	1.6	9.1
	5. Oceanic equatorial [%]	13.0	11.9	14.9	11.7
	5. Oceanic equatorial [mm/month]	16.7	16.1	6.9	33.5
	6. Oceanic south [%]	18.0	20.8	18.6	21.8
	6. Oceanic south [mm/month]	22.5	31.6	8.1	69.7
Continental evaporative contribution [%]		21.9	24.0	16.4	30.6
Continental evaporative contribution [mm/month]		29.4	45.9	7.1	94.7
Other [%]		14.6	12.3	13.2	12
Other [mm/month]		18.8	19.3	5.9	28.2
September				**(1997, 2002, 2006)**	**(2013, 2017, 2021)**
Oceanic evaporative contribution					
	1. Coastal equatorial [%]	9.8	8.9	9.5	9.1
	1. Coastal equatorial [mm]	5.6	8.7	2.2	12.8
	2. Coastal south [%]	4.4	4.9	4.1	5.1
	2. Coastal south [mm/month]	2.6	4.9	1.0	7.1
	3. Oceanic north Madagascar [%]	12.0	10.6	13.8	10.6
	3. Oceanic north Madagascar [mm/month]	6.7	10.3	3.0	14.9
	4. Oceanic east Madagascar [%]	30.7	28.0	36.8	28.8
	4. Oceanic east Madagascar [mm/month]	17.5	27.6	8.1	40.9
	5. Oceanic far east [%]	13.1	8.7	16.1	11.6
	5. Oceanic far east [mm/month]	7.1	8.8	3.4	16.6
Continental evaporative contribution [%]		27.6	29.8	17.4	28.4
Continental evaporative contribution [mm/month]		17.4	29.1	4.1	40.5
Other [%]		3.6	9.3	2.5	6.7
Other [mm/month]		2.1	7.9	0.5	9.2

0.48 (p=0.12). Oceanic evaporation contributes to 70 % (40 mm/month) prior to 2010 and 61 % (60 mm/month) post 2010, representing a 20 mm/month difference and 50 % increase. Figure S4 visualizes the overall moisture source for September.

Continental evaporation became more intense around the West of the catchment region and there is a high concentration of evaporative contribution around the catchment that contributes to the precipitation. Regarding oceanic moisture, intensification is observed along the coast between Madagascar and Mozambique. An extension of evaporative contribution is observed towards the South and East in the Indian Ocean (see Figure S5).

For September five regions can be distinguished as oceanic moisture sources, as listed in Table 1 and visualized in Figure S3. It becomes evident that the oceanic region 4 evaporative contribution is highest with 31 % before 2010 and 28 % after. After 2010, the distribution has slightly shifted, with, most notably, the reduction in percentage contribution of region 5 from 13 % to 9 % and the increase of oceanic region 2 from 4 % to 5 %. As September precipitation generally increases after the change point, the evaporative contribution for all sea regions increases as well. The absolute increase is most profound in sea region 4 from 18 mm/month to 28 mm/month representing a 56 % increase.

The three lowest and highest precipitation months for September are investigated as well for their moisture sources and evaporative contribution. The three driest years include 1997, 2002, and 2006, with 22 mm/month on average. The three wettest September months include 2013, 2017 and 2021, with 142 mm/month on average (see Table 1). The precipitation increment is 545 % while continental evaporative contribution represents a 890 % increment. The three driest years have an continental evaporative contribution of 17 % (4 mm/month) opposed to 28 % (41 mm/month) in the three wettest years. All regions, except for region 2, show a decrease in their relative contribution.

3.3 Sea surface temperature

SST is an important metric for the rate of evaporation from the sea surface. The spatial plots in Figure 3 reveal a more positive SST anomaly in the southern Indian Ocean compared to the northern Indian Ocean. When we compare the areas for which 50 % of the evaporated moisture has been tracked, we notice that the location of the evaporative contribution has shifted towards the area where SST have increased most. This concerns especially the region between Mozambique and Madagascar, and east of Madagascar.

The decadal SST anomaly reveals that SST has mainly risen in two most recent decades. Between 1989 and 1999, April SST remained stable below the equator, while increasing 0.2°C above the equator. SST below the equator declined by 0.1°C to 0.3°C for the month September. Regarding 2000 to 2009, SST has increased mainly at 30° S with up to 0.35°C for the month April and an increasing SST from the equator towards the north between 0°C and 0.4°C. The moisture source for September precipitation does not reach North of the equator. South of the equator SST increased between 0.1°C and 0.2°C. The main increase in SST happened in the most recent decade from 2010 to 2021 where SST in April reached 0.2°C to 0.4°C warming. The positive SST anomaly for September shifts over 0.4°C from 30° S to 20° S of over 0.4°C. The main increase in SST for both months happened between 10° S and 30° S. For the April and September precipitation to ocean region SST Pearson correlation see Table S5 to S6.

4 Discussion

The precipitation regime after 2010 shows distinct behavior as it shows a uni-modal rather than the bi-modal annual precipitation cycle before 2010. The long rainy season from March to May is very strong, whereas the short rains season from October to December does not show a second major jump. The change point in 2010 indicates a change in precipitation regime for the catchment with April and September precipitation surging the most. Cook and Vizy (2013) suggested that as a result of climate change the short rains season could be lengthened. The increase in September to third highest precipitation month, preceding the actual short rainy season, corroborates this.

The catchment represents a higher than expected relative continental evaporative contribution. Keys et al. (2022) found that on average 85 % of Kenya's annual precipitation consists of moisture from oceanic evaporation and 15 % from continental evaporation. This study found that continental evaporation can have a significantly larger contribution of about 29 % in the month of April and 32 % for September precipitation. Extremes are found with continental contributions of over 40 %.

In case of a warming world, Findell et al. (2019) found that the ratio between oceanic and continental evaporation would become larger, making oceanic evaporation more important for land precipitation in general. We found that continental evaporation became relatively more important compared to oceanic evaporation. This could be explained by the absolute increase in evaporative contribution from the ocean. As a result, more water is available for continental evaporation.

Regarding SST, the main focus was on the trend rather than a change point. No change points were found, but an increasing SST trend has been observed. This is in line with several studies suggesting a future warming of the Indian Ocean (Sharma et al., 2023; Roxy et al., 2020), a possible increase in extreme precipitation over Kenya (Endris et al., 2019), and the relation between Indian Ocean temperatures and East African rainfall (Ummenhofer et al., 2009). Given the results of this study, it is likely that as a result of changing SST, the resulting moisture source shift to a warmer parts of the Indian Ocean and the implication on precipitation, lake Nakuru water levels could potentially experience more lake water level rise phenomena in the future.

This method of investigating precipitation variability and evaporative contributions of the moisture sources produces interesting insights into the changing climatology of the catchment and could be applied to more catchments in the Rift Valley to investigate possible similarities and differences. The study employed a novel method to investigate changes in the precipitation regimes on a small scale by combining moisture source, evaporative contribution, and SST. It would be stimulating to investigate other climate entities like wind patterns, ocean flow, and El Niño.

5 Conclusions

The objective of this research was to gain insights into the main drivers responsible for the rising water levels of Lake Nakuru. Specifically, the aim was to test the premise that increased precipitation in the catchment was caused by a change in moisture source, especially the evaporative contribution and sea surface temperature as climatic drivers. We have investigated the spatial and temporal variability of precipitation in the lake Nakuru catchment by validating change points and relating this variability to lake levels. The origin and underlying causes for this variability in precipitation were evaluated by applying moisture tracking with the WAM2layers model to identify moisture sources and changes in evaporative contributions.

Change points in precipitation were confirmed in catchment and lake precipitation for the majority of weather stations in 2010. Notably, this change point coincides with the rise in lake volume from 2010 onward (see Figure 2). Catchment precipitation has increased with about 19 % while several weather stations show more precipitation of up to 48 %. The months of April and September together contribute 46 % of the total annual increase in precipitation over the catchment, which is further substantiated by the change point in September precipitation.

Moisture tracking revealed that over time, the western Indian Ocean region East of Madagascar became an increasingly important moisture source for precipitation in both April and September (see Figure 3). This was tied to a more than average SST increase in this specific region. We also found that moisture was produced more locally after the change point with also an increased continental evaporation contribution.

In conclusion, the results of this study strongly suggest that the rise of water levels of Lake Nakuru and associated flooding is likely to be attributed to increased precipitation, especially in April and September. Utilizing an atmospheric moisture tracking model, our study revealed that this transformation in precipitation regime is associated with a southward shift in moisture sources. More moisture is now coming from the southern Indian Ocean, where substantial increases in sea surface temperatures and evaporation are observed.

Open Research Section

Kenya Meteorological Department precipitation data can be requested through `https://meteo.go.ke/resources/data-request`. Time series of lake characteristics can be obtained through `https://dahiti.dgfi.tum.de/en/13220/surface-area/`. The code for WAM2layers moisture tracking model is provided at `https://github.com/WAM2layers/WAM2layers`. ERA5 reanalysis data on hourly basis can be downloaded from `https://cds.climate.copernicus.eu/cdsapp#!/dataset/reanalysis-era5-single-levels?tab=overview`. Sea surface temperature data can be retrieved via `https://cds.climate.copernicus.eu/cdsapp#!/dataset/reanalysis-oras5?tab=overview`.

Acknowledgments

This research has been supported by the European Horizon Europe Programme under grant agreement nr. 101086209 (TEMBO Africa). We thank the Kenya Meteorological Department for providing rainfall data.

References

Balagizi, C. M., Kasereka, M. M., Cuoco, E., & Liotta, M. (2018). Influence of moisture source dynamics and weather patterns on stable isotopes ratios of precipitation in central-eastern africa. *Science of the Total Environment*, *628*, 1058–1078.

Benedict, I., van Heerwaarden, C. C., van der Ent, R. J., Weerts, A. H., & Hazeleger, W. (2020, feb). Decline in Terrestrial Moisture Sources of the Mississippi River Basin in a Future Climate. *Journal of Hydrometeorology*, *21*(2), 299–316. doi: 10.1175/JHM-D-19-0094.1

Black, E. (2005). The relationship between indian ocean sea–surface temperature and east african rainfall. *Philosophical Transactions of the Royal Society A: Mathematical, Physical and Engineering Sciences*, *363*(1826), 43–47.

Black, E., Slingo, J., & Sperber, K. R. (2003). An observational study of the relationship between excessively strong short rains in coastal east africa and indian ocean sst. *Monthly Weather Review*, *131*(1), 74–94.

Carr, T., & Ummenhofer, C. C. (2023, oct). Impact of atmospheric circulation variability on U.S. Midwest moisture sources. *Journal of Climate*, 1–41. Retrieved from `https://journals.ametsoc.org/view/journals/clim/aop/JCLI-D-23-0178.1/JCLI-D-23-0178.1.xml` doi: 10.1175/JCLI-D-23-0178.1

Cook, K. H., & Vizy, E. K. (2013). Projected changes in east african rainy seasons. *Journal of Climate*, *26*(16), 5931–5948.

Copernicus. (2021). *Oras5 global ocean reanalysis monthly data from 1958 to present.* Copernicus Climate Change Service (C3S) Climate Data Store (CDS). Retrieved 31/03/2023, from `https://cds.climate.copernicus.eu/cdsapp#`

!/dataset/reanalysis-oras5?tab=overview doi: 10.24381/cds.67e8eeb7
Duerinck, H. M., van der Ent, R. J., van de Giesen, N. C., Schoups, G., Babovic, V., & Yeh, P. J.-F. (2016). Observed Soil Moisture-Precipitation Feedback in Illinois: A Systematic Analysis over Different Scales. *Journal of Hydrometeorology*, *16*(6), 1645–1660. doi: 10.1175/JHM-D-15-0032.1
Dyer, E., & Washington, R. (2021). Kenyan long rains: A subseasonal approach to process-based diagnostics. *Journal of Climate*, *34*(9), 3311–3326.
Endris, H. S., Lennard, C., Hewitson, B., Dosio, A., Nikulin, G., & Artan, G. A. (2019). Future changes in rainfall associated with enso, iod and changes in the mean state over eastern africa. *Climate dynamics*, *52*, 2029–2053.
ERA5. (2017). Copernicus climate change service (c3s)(2017): Era5: Fifth generation of ecmwf atmospheric reanalyses of the global climate. copernicus climate change service climate data store (cds).
Findell, K. L., Keys, P. W., Van der Ent, R. J., Lintner, B. R., Berg, A., & Krasting, J. P. (2019). Rising temperatures increase importance of oceanic evaporation as a source for continental precipitation. *Journal of Climate*, *32*(22), 7713–7726.
Gichuru, G., & Waithaka, H. (2016). Analysis of lake nakuru surface water area variations using geospatial technologies. In *Scientific conference proceedings.*
Guo, L., van der Ent, R. J., Klingaman, N. P., Demory, M.-E., Vidale, P. L., Turner, A. G., ... Chevuturi, A. (2019, apr). Moisture Sources for East Asian Precipitation: Mean Seasonal Cycle and Interannual Variability. *Journal of Hydrometeorology*, *20*(4), 657–672. Retrieved from http://journals.ametsoc.org/doi/10.1175/JHM-D-18-0188.1 doi: 10.1175/JHM-D-18-0188.1
Herrnegger, M., Stecher, G., Schwatke, C., & Olang, L. (2021). Hydroclimatic analysis of rising water levels in the great rift valley lakes of kenya. *Journal of Hydrology: Regional Studies*, *36*, 100857.
Hersbach, B. B. B. P. B. G. H. A. M. S. J. N. J. P. C. R. R. R. I. S. D. S. A. S. C. D. D. T. J.-N., H. (2023). *Era5 hourly data on single levels from 1940 to present.* Copernicus Climate Change Service (C3S) Climate Data Store (CDS). doi: 10.24381/cds.adbb2d47
ilec. (2005). Managing lakes and their basins for sustainable use: A report for lake basin managers and stakeholders.
Iradukunda, P., Sang, J. K., Nyadawa, M. O., & Maina, C. W. (2020). Sedimentation effect on the storage capacity in lake nakuru, kenya. *Journal of Sustainable Research in Engineering*, *5*(3), 149–158.
Keim, B. D., & Muller, R. A. (1992). Temporal fluctuations of heavy rainfall magnitudes in new orleans, louisiana: 1871–1991 1. *JAWRA Journal of the American Water Resources Association*, *28*(4), 721–730.
Keys, P. W., Warrier, R., Van der Ent, R. J., Galvin, K. A., & Boone, R. B. (2022). Analysis of kenya's atmospheric moisture sources and sinks. *Earth Interactions*, *26*(1), 139–150.
Kimaru, A. N., Gathenya, J. M., & Cheruiyot, C. K. (2019). The temporal variability of rainfall and streamflow into lake nakuru, kenya, assessed using swat and hydrometeorological indices. *Hydrology*, *6*(4), 88.
KMD. (2022). *Precipitation daily data in lake nakuru catchment from kenya meteorological department.*
Levin, N. E., Zipser, E. J., & Cerling, T. E. (2009). Isotopic composition of waters from ethiopia and kenya: Insights into moisture sources for eastern africa. *Journal of Geophysical Research: Atmospheres*, *114*(D23).
Liang, L., Li, L., & Liu, Q. (2011). Precipitation variability in northeast china from 1961 to 2008. *Journal of Hydrology*, *404*(1-2), 67–76.
Liu, Y., Zhang, C., Tang, Q., Hosseini-Moghari, S.-M., Haile, G. G., Li, L., ... Chen, D. (2021, aug). Moisture source variations for summer rainfall in different intensity classes over Huaihe River Valley, China. *Climate Dynamics*, *57*(3-4), 1121–1133. Retrieved from https://doi.org/10.1007/s00382-021-05762-4https://link.springer.com/10.1007/s00382-021-05762-4 doi: 10.1007/s00382-021-05762

-4
McKnight, P. E., & Najab, J. (2010). Mann-whitney u test. *The Corsini encyclopedia of psychology*, 1–1.
Odada, E. (2001). Stable isotopic composition of east african lake waters.
Roxy, M., Gnanaseelan, C., Parekh, A., Chowdary, J. S., Singh, S., Modi, A., … others (2020). Indian ocean warming. *Assessment of Climate Change over the Indian Region: A Report of the Ministry of Earth Sciences (MoES), Government of India*, 191–206.
Schumann, A. (1998). *Encyclopedia of hydrology and lakes. encyclopedia of earth science.* Springer: Dordrecht, The Netherlands.
Schwatke, C., Scherer, D., & Dettmering, D. (2019). Automated extraction of consistent time-variable water surfaces of lakes and reservoirs based on landsat and sentinel-2. *Remote Sensing*, *11*(9), 1010.
Sharma, S., Ha, K.-J., Yamaguchi, R., Rodgers, K. B., Timmermann, A., & Chung, E.-S. (2023). Future indian ocean warming patterns. *Nature Communications*, *14*(1), 1789.
The World Bank Group. (2021). *Kenya current climate ¿ climateology. observed average annual precipitation of kenya for 1901-2020.*
Truong, C., Oudre, L., & Vayatis, N. (2020). Selective review of offline ch ange point detection methods. *Signal Processing*, *167*, 107299.
Ummenhofer, C. C., Gupta, A. S., England, M. H., & Reason, C. J. (2009). Contributions of indian ocean sea surface temperatures to enhanced east african rainfall. *Journal of climate*, *22*(4), 993–1013.
Van der Ent, R., Benedict, I., Weijenborg, C., Cömert, T., van de Koppel, N., Guo, L., & Kalverla, P. (2022, March 18). *Wam2layers.* Zenodo. doi: 10.5281/zenodo.7010594
Van der Ent, R. J., & Savenije, H. H. G. (2013). Oceanic sources of continental precipitation and the correlation with sea surface temperature. *Water Resources Research*, *49*(7), 3993–4004.
Van der Ent, R. J., Wang-Erlandsson, L., Keys, P. W., & Savenije, H. H. G. (2014). Contrasting roles of interception and transpiration in the hydrological cycle–part 2: Moisture recycling. *Earth System Dynamics*, *5*(2), 471–489.
Yang, W., Seager, R., Cane, M. A., & Lyon, B. (2015). The annual cycle of east african precipitation. *Journal of Climate*, *28*(6), 2385–2404.

Supporting Information for "Rising water levels of Lake Nakuru, Kenya: Unraveling the Changing Precipitation Regime and its Climatic Drivers"

R. Ampting[1], R. van der Ent[1], V. Kiluva[2], N. van de Giesen[1]

[1]Delft University of Technology, The Netherlands

[2]Masinde Muliro University of Science and Technology, Kenya

Contents of this file

1. Tables S1 to S6
2. Figures S1 to S5

Additional Supporting Information can be found here: `https://data.4tu.nl/private_datasets/Yzm7TvL_uDLVd6qV3kFHKqSjP5yXmHAMxLM4wGPvtnM`

1. Precipitation and Lake Analysis.ipynb
2. Moisture Source and SST April.ipynb
3. Moisture Source and SST September.ipynb
4. Moisture tracking output April.zip
5. Moisture tracking output September.zip
6. SST_month_avg_82_21.nc

Introduction

The research relies on precipitation data from the Kenya Meteorological Department (KMD) collected between 1981 and 2021. The data cover fourteen weather stations situated across the catchment area, and there are no apparent gaps in the data. The data is processed with the Thiessen polygon method to extract mean catchment precipitation. Two datasets are used to understand lake behavior: the Database for Hydrological Time Series of Inland Waters (DAHITI) and a bathymetry study conducted by Jomo Kenyatta University of Agriculture and Technology (JKUAT). DAHITI provides surface area time series data, while the bathymetry study informs the relationship between lake volume and surface area. The two data sets are combined to obtain the volume time series of the lake. The research employs the WAM2layers moisture tracking model, which requires input data on surface and model-level variables. ERA5 hourly data, covering a specific geographical domain and time period, is used for this purpose. Sea surface temperature data from the European Center for Medium-Range Weather Forecasts are utilized to assess the influence of different moisture sources. These data cover a global range and is extracted for 1981 to 2021.

Table S1. Fourteen weather stations from the Kenya Meteorological Department from 1981 to 2021. The area weight is determined with the Thiessen polygon method in QGIS.

Station	Latitude [S]	Longitude [E]	Elevation [m amsl]	Mean rainfall [mm/year]	Area weight [%]
Pts2	-0.4433	35.8903	2600	1123	5.2
Pts3	-0.3616	35.9595	2166	987	7.2
Pts4	-0.4521	35.9584	2380	979	6.1
Pts5	-0.5569	35.9432	2756	1050	8.3
Pts6	-0.3032	36.0432	1817	905	8.6
Pts7	-0.4002	36.0436	1951	915	7.3
Pts8	-0.5017	36.0482	2022	815	8.5
Pts9	-0.6143	36.0497	2564	810	11.3
Pts10	-0.2811	36.1231	1860	901	12.0
Pts11	-0.3991	36.1489	1845	1004	6.5
Pts12	-0.5172	36.1505	1838	719	7.9
Pts13	-0.6374	36.1596	2305	845	6.0
Pts14	-0.6253	36.2014	2352	912	2.7
Pts15	-0.4102	36.1805	1893	835	2.3

Table S2. Change point detection results for weather stations 2 to 15, lake precipitation, and catchment precipitation. Eight out of fourteen weather stations experience a significant change point at 2010. Lake precipitation experiences a significant change point at 2010, however for the catchment precipitation average precipitation does not reach below 0.05 significance level.

Time series	Elevation [m]	P_pre2010 [mm]	P_post2010 [mm]	Change [mm]	Change [%]	Change_Point	Significance
Pts2	2600	1040.21	1322.67	282.46	27.15%	2010	0.0007
Pts3	2166	916.82	1157.42	240.6	26.24%	2010	0.0040
Pts4	2380	925.79	1106.96	181.17	19.57%	-	0.0882
Pts5	2756	1011.53	1142.85	131.32	12.98%	-	0.1479
Pts6	1817	855.01	1024.64	169.63	19.84%	2010	0.0195
Pts7	1951	869.65	1024.82	155.17	17.84%	-	0.0605
Pts8	2022	816.97	811.48	-5.49	-0.67%	-	0.5191
Pts9	2564	813.22	802.75	-10.47	-1.29%	-	0.4307
Pts10	1860	850.42	1021.58	171.16	20.13%	2010	0.0211
Pts11	1845	895.9	1266.31	370.41	41.35%	2010	0.0000
Pts12	1838	680.91	811.63	130.72	19.20%	2010	0.0122
Pts13	2305	786.5	985.07	198.57	25.25%	2010	0.0048
Pts14	2352	800.04	1182.03	381.99	47.75%	2010	0.0000
Pts15	1893	773.08	986.56	213.48	27.61%	2010	0.0008
Lake_Precipitation	1868	871.26	1090.65	219.39	25.18%	2010	0.0068
Catchment_Precipitation	2168	849.11	1005.05	145.51	18.37%	2010	0.0434

Table S3. Change point detection results for monthly mean catchment precipitation. September and October experience a significant change point at 2010.

Time series	P_pre2010	P_post2010	Change [mm]	Change [%]	Percent of total change (%)	Change_Point	Significance
Jan	36.27	28.67	-7.60	-20.96%	-5.22%	-	0.4307
Feb	30.97	30.48	-0.49	-1.59%	-0.34%	-	1
Mar	65.90	74.65	8.75	13.28%	6.02%	-	0.7635
Apr	125.47	159.13	33.66	26.83%	23.13%	-	0.3667
May	94.50	117.57	23.07	24.41%	15.85%	-	0.1400
Jun	71.53	77.85	6.31	8.82%	4.34%	-	0.6569
Jul	72.44	86.28	13.84	19.11%	9.51%	-	0.2343
Aug	91.77	93.60	1.83	2.00%	1.26%	-	0.57633
Sep	58.65	96.46	37.81	64.46%	25.98%	2010	0.0036
Oct	66.67	87.81	21.14	31.71%	14.53%	2010	0.0328
Nov	82.34	84.02	1.68	2.04%	1.15%	-	0.9657
Dec	52.61	68.56	15.96	30.33%	10.96%	-	0.4476

Table S4. Monthly precipitation and total monthly volume change accompanied by their Pearson correlation for the years 2009 to 2021.

Month	Precipitation [mm/month]	Accumulated contribution to the total volume [km^3]	Pearson correlation [-]	p-value [-]
Jan	27	0.004	0.24	0.42
Feb	29	-0.024	0.67	0.01
Mar	70	-0.012	0.48	0.09
Apr	152	0.062	0.82	0.00
May	118	0.062	0.26	0.39
Jun	74	0.033	0.63	0.02
Jul	81	0.034	0.13	0.67
Aug	89	0.045	0.48	0.09
Sep	92	0.053	0.53	0.06
Oct	85	-0.010	-0.03	0.92
Nov	81	0.022	0.65	0.02
Dec	73	0.030	0.41	0.17

Table S5. Correlation of April SST from regions with April precipitation over a one year, three year, six year, and nine year mean

Region	Correlation 1 year	Prior 2010 1 year	Post 2010 1 year	Correlation 3 year	Prior 2010 3 year	Post 2010 3 year	Correlation 6 year	Prior 2010 6 year	Post 2010 6 year	Correlation 9 year	Prior 2010 9 year	Post 2010 9 year
1	0.19	0.26	-0.08	0.10	-0.05	-0.09	0.02	-0.33	0.72 (p=0.01)	-0.19	-0.59 (p=0.00)	0.42
2	-0.06	-0.02	-0.42	0.03	-0.06	-0.00	0.15	-0.01	0.66 (p=0.02)	-0.04	-0.23	0.34
3	0.21	0.17	0.15	0.38 (p=0.02)	0.21	0.39	0.33 (p=0.05)	-0.15	0.88 (p=0.00)	0.30	-0.31	0.88 (p=0.00)
4	0.32 (p=0.04)	0.34	0.15	0.22	0.07	-0.04	0.17	-0.41	0.93 (p=0.00)	0.01	-0.63 (p=0.00)	0.76 (p=0.00)
5	-0.05	-0.01	-0.56	0.20	-0.19	-0.00	0.28	-0.27	0.86 (p=0.00)	0.21	-0.38	0.84 (p=0.00)
6	0.22	0.16	0.15	0.35 (p=0.03)	0.25	0.18	0.42 (p=0.01)	-0.11	0.89 (p=0.00)	0.35 (p=0.05)	-0.2	0.87 (p=0.00)
All	0.18	0.21	-0.10	0.26	0.05	0.10	0.26	-0.25	0.90	0.11	-0.47	0.82

Table S6. Correlation of September SST from regions with September precipitation over a one year, three year, six year, and nine year rolling mean period

Region	Correlation 1 year	Prior 2010 1 year	Post 2010 1 year	Correlation 3 year	Prior 2010 3 year	Post 2010 3 year	Correlation 6 year	Prior 2010 6 year	Post 2010 6 year	Correlation 9 year	Prior 2010 9 year	Post 2010 9 year
1	0.11	-0.15	-0.12	0.60 (p=0.00)	0.09	0.61 (p=0.04)	0.65 (p=0.00)	-0.32	0.21	0.71 (p=0.00)	-0.51 (p=0.02)	0.65 (p=0.02)
2	-0.04	-0.04	-0.72 (p=0.01)	0.19	-0.20	-0.44	0.38 (p=0.02)	-0.38	-0.02	0.49 (p=0.00)	-0.57 (p=0.01)	0.21
3	0.15	-0.08	0.02	0.57 (p=0.00)	0.18	0.16	0.63 (p=0.00)	-0.30	-0.41	0.70 (p=0.00)	-0.42	0.34
4	0.17	-0.13	-0.20	0.60 (p=0.00)	0.06	0.05	0.73 (p=0.00)	-0.14	0.54	0.81 (p=0.00)	-0.16	0.87 (p=0.00)
5	0.37 (p=0.02)	-0.00	-0.12	0.67 (p=0.00)	0.05	-0.11	0.83 (p=0.00)	-0.05	0.78 (p=0.00)	0.88 (p=0.00)	-0.12	0.90 (p=0.00)
All	0.18	-0.11	-0.33	0.60 (p=0.00)	0.04	0.04	0.70 (p=0.00)	-0.27	0.47	0.76 (p=0.00)	-0.40	0.87 (p=0.00)

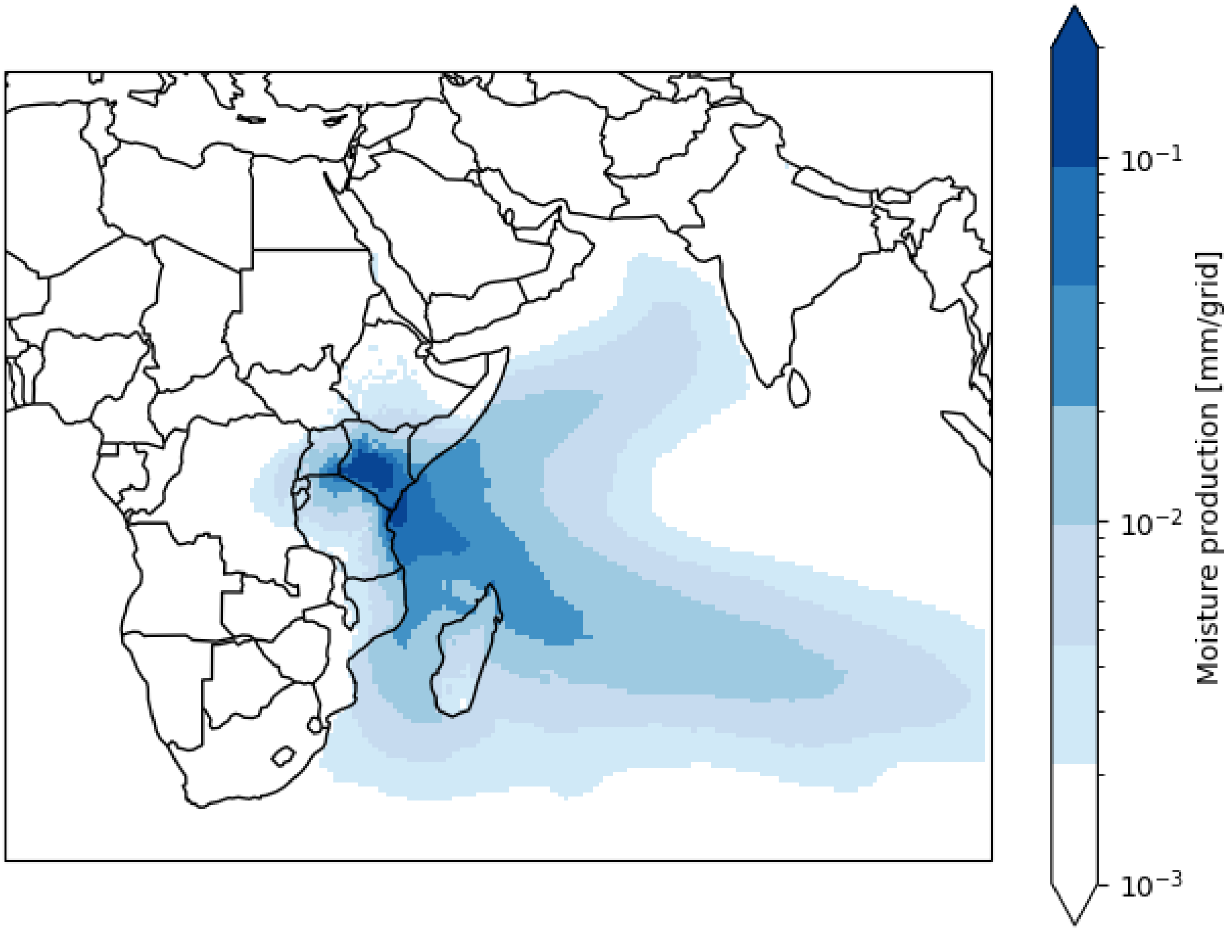

Figure S1. Moisture source for the month of April on average between 1981 and 2021

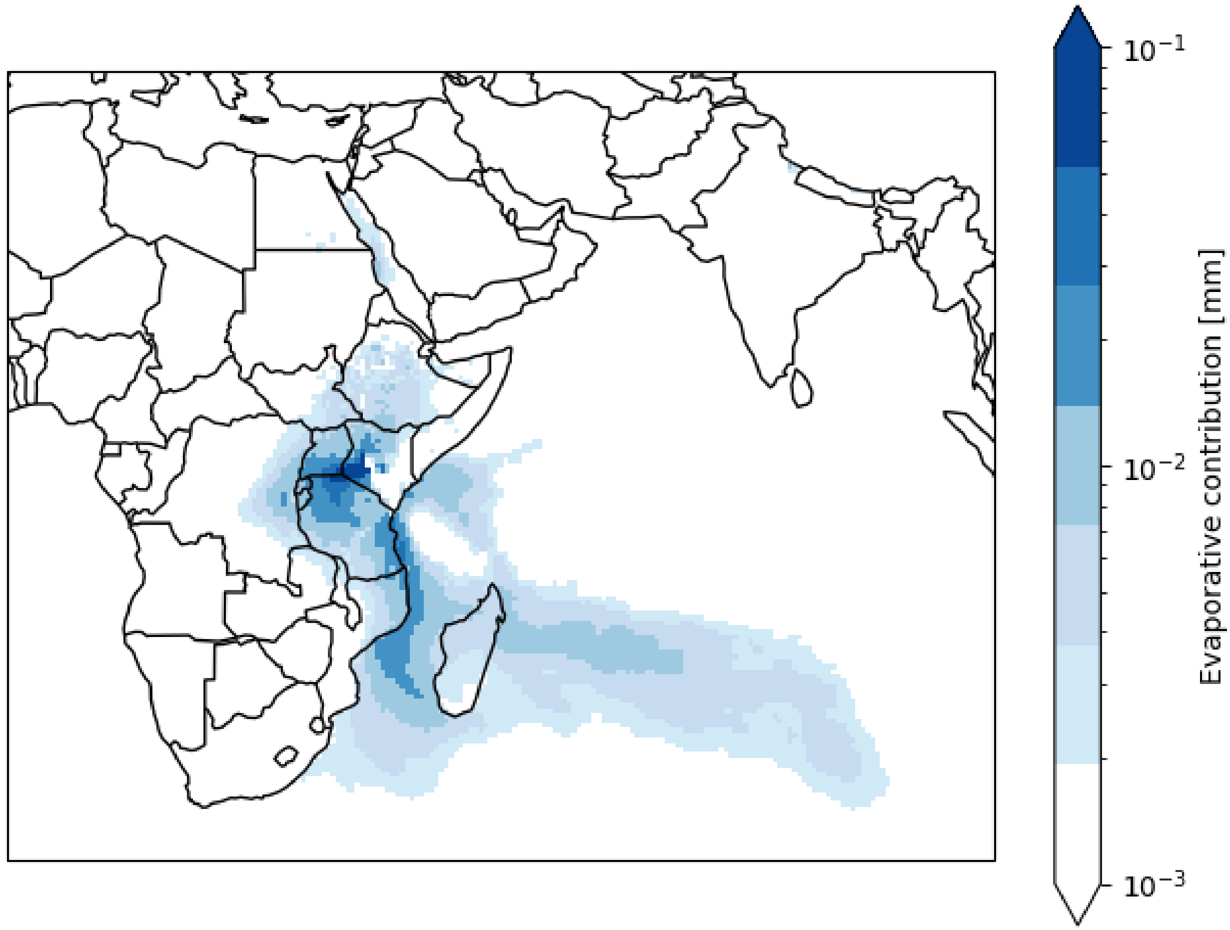

Figure S2. April evaporative contribution difference between 1981 to 2009 and 2010 to 2021

(a) April

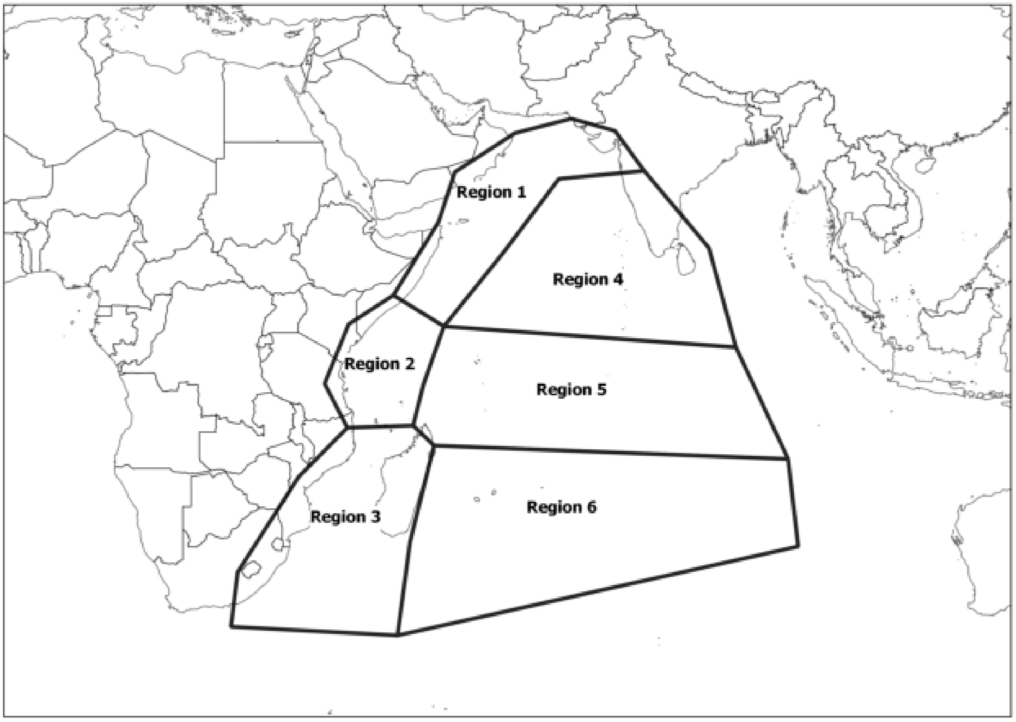

(b) September

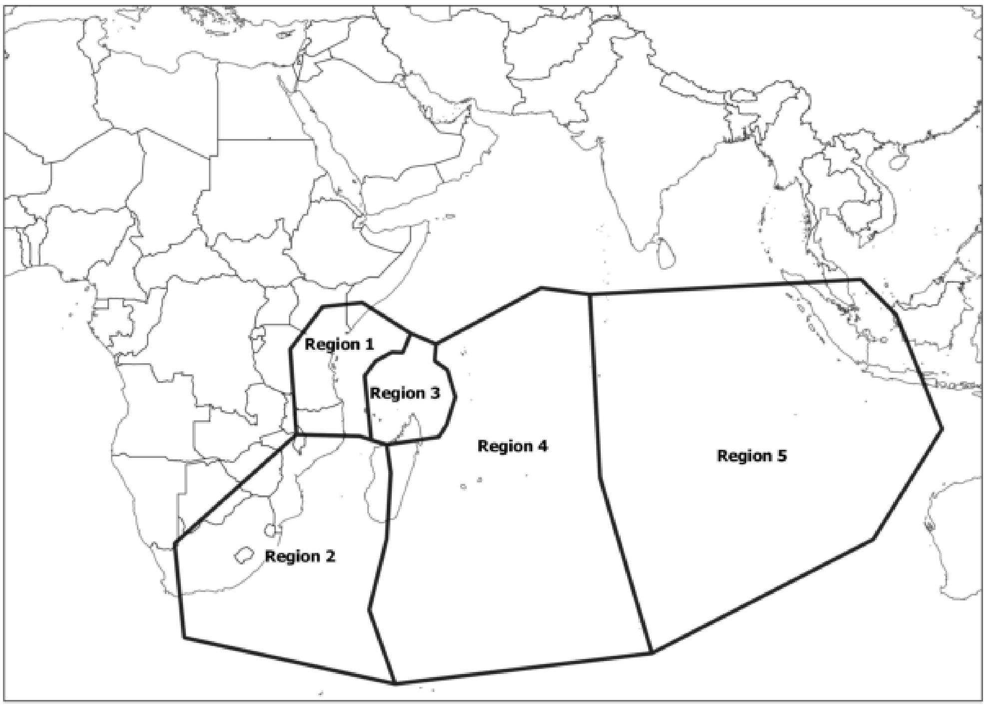

Figure S3. Location of the oceanic regions

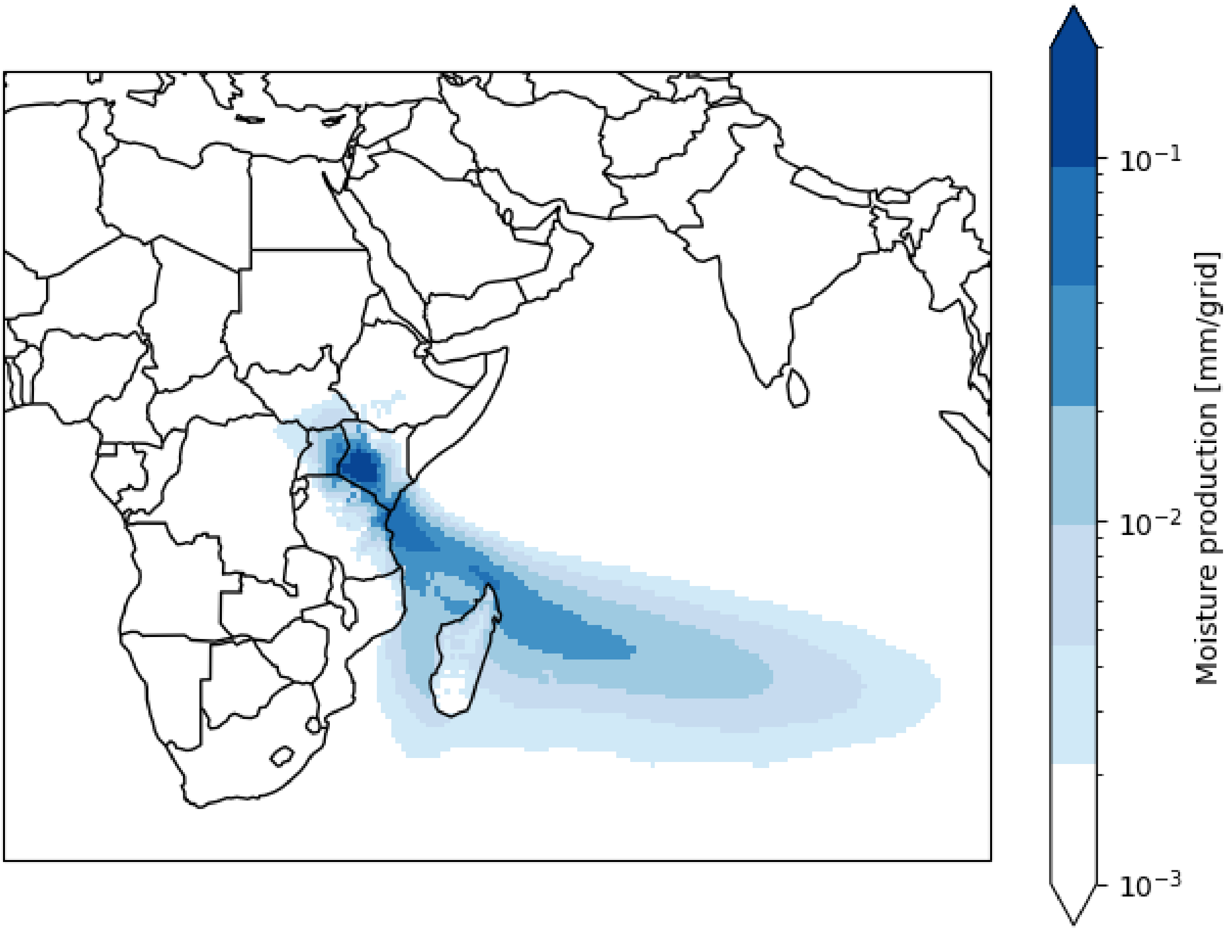

Figure S4. Moisture source for the month of September on average between 1981 and 2021

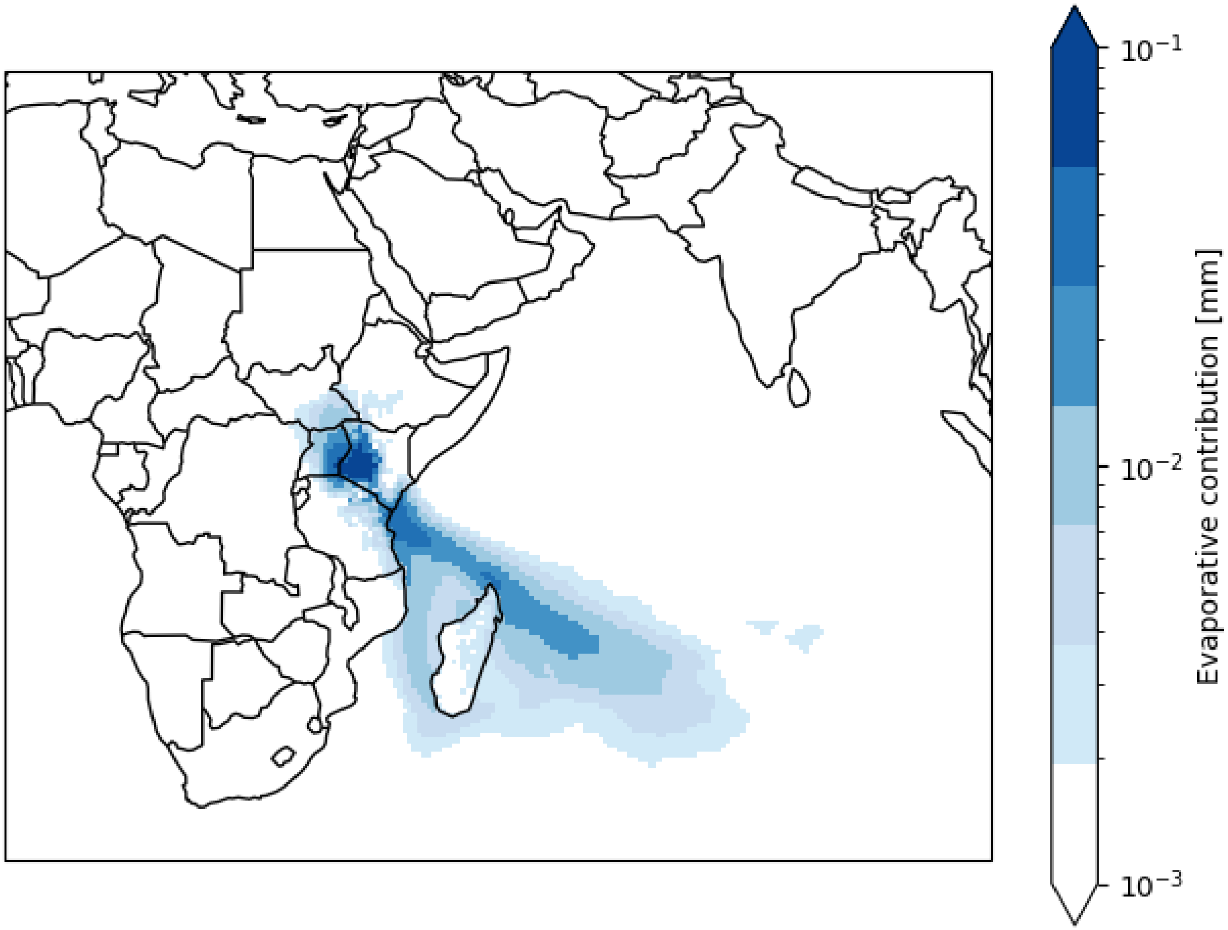

Figure S5. September evaporative contribution difference between 1981 to 2009 and 2010 to 2021